

1 Anomalous Amide Proton Chemical Shifts as Signatures of Hydrogen 2 Bonding to Aromatic Sidechains

3 Kumaran Baskaran*¹, Colin W. Wilburn*¹, Jonathan R. Wedell¹, Leonardus M. I. Koharudin², Eldon L.
4 Ulrich¹, Adam D. Schuyler¹, Hamid R. Eghbalnia¹, Angela M. Gronenborn², and Jeffrey C. Hoch¹

5 ¹Department of Molecular Biology and Biophysics, UConn Health, 263 Farmington Ave., Farmington, CT 06030-3305 USA

6 ²Department of Structural Biology University of Pittsburgh School of Medicine 3501 Fifth Ave., BST3/Rm. 1050 Pittsburgh, PA
7 15260 USA

8 *Correspondence to:* Jeffrey C. Hoch (hoch@uchc.edu)

9 Dedicated to Professor Robert Kaptein on the occasion of his 80th birthday.

10 **Abstract.** Hydrogen bonding between an amide group and the p- π cloud of an aromatic ring was first identified in a protein in the
11 1980s. Subsequent surveys of high-resolution X-ray crystal structures found multiple instances, but their preponderance was
12 determined to be infrequent. Hydrogen atoms participating in a hydrogen bond to the p- π cloud of an aromatic ring are expected
13 to experience an upfield chemical shift arising from a shielding ring current shift. We survey the Biological Magnetic Resonance
14 Data Bank for amide hydrogens exhibiting unusual shifts as well as corroborating nuclear Overhauser effects between the amide
15 protons and ring protons. We find evidence that Trp residues are more likely to be involved in p- π hydrogen bonds than other
16 aromatic amino acids, whereas His residues are more likely to be involved in in-plane hydrogen bonds with a ring nitrogen acting
17 as the hydrogen acceptor. The p- π hydrogen bonds may be more abundant than previously believed. The inclusion in NMR structure
18 refinement protocols of shift effects in amide protons from aromatic side chains, or explicit hydrogen bond restraints between
19 amides and aromatic rings, could improve the local accuracy of side-chain orientations in solution NMR protein structures, but
20 their impact on global accuracy is likely be limited.

21 1 Introduction

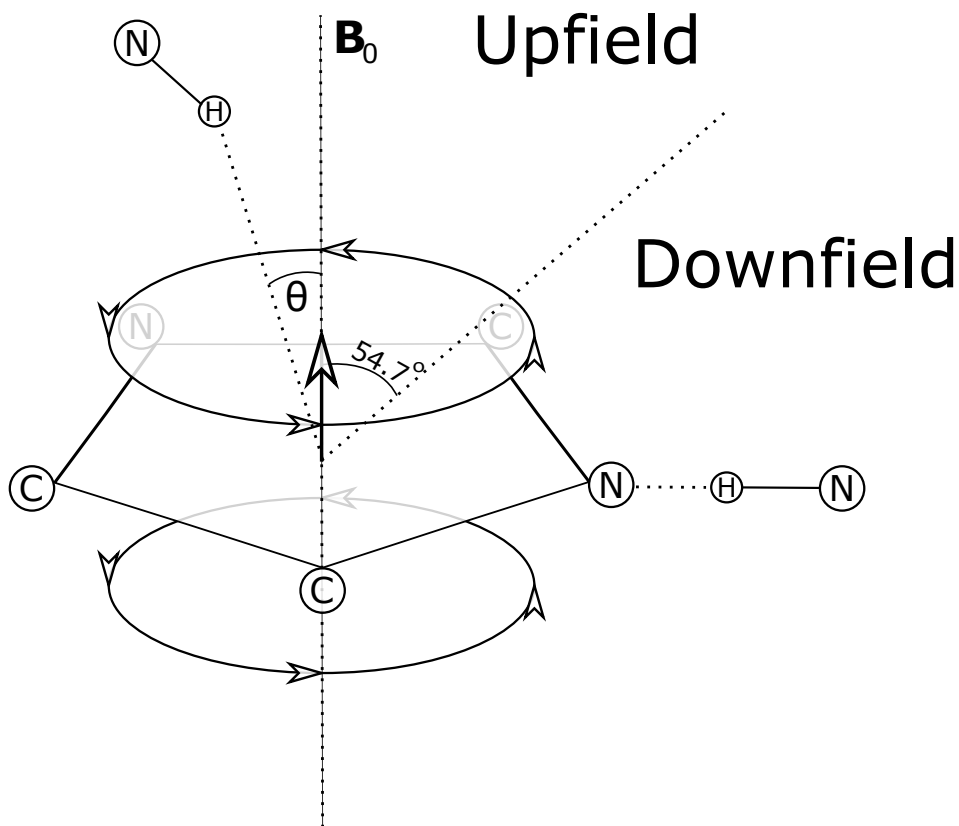
22 In 1986, Perutz et al.(Levitt and Perutz, 1988) identified a putative hydrogen bond between an amino group of Asparagine and an
23 aromatic ring of a drug bound to hemoglobin. Similar observations of the π electrons of aromatic rings acting as acceptors for
24 hydrogen bonding have been reported before and since.(Klemperer et al., 1954; Mcphail and Sim, 1965; Knee et al., 1987) Later
25 in 1986, Burley and Petsko (Burley and Petsko, 1986) surveyed 33 high resolution protein structures and found further evidence
26 of aromatic hydrogen bonds. Tüchsen and Woodward (Tüchsen and Woodward, 1987) subsequently observed an upfield shift in
27 the Gly-37 NH and Asn-44 HN resonances due to a nearby Tyr-35 aromatic group. The measurements from this study allowed
28 Levitt and Perutz (Perutz, 1993) to estimate that these interactions contribute around 3 kcal mol⁻¹ in stabilizing enthalpy, about
29 half as strong as a conventional hydrogen bond. Further evidence of such H-bonding came from the 2001 study by Brinkley and
30 Gupta (Brinkley and B., 2001) showing FTIR spectroscopic evidence for hydrogen bonding between alcohols and aromatic rings.
31 The ability of aromatic rings to engage in weakly polar CH- π interactions is well documented, with NMR data from Plevin et
32 al.(Plevin et al., 2010) in the form of weak scalar (J) couplings between methyl groups and atoms in aromatic rings providing direct
33 evidence of these interactions. The study also included a survey of 183 X-ray structures and found 183 putative Me/ π interactions.
34 Brandl et al.(Brandl et al., 2001) surveyed 1154 protein structures from the Protein Data Bank (PDB (Consortium, 2019) for C-H

35 π H bonds and found 14,087 involving aromatic rings and satisfying their geometric criteria. This is made all the more impressive
36 when considering that Levitt and Perutz report the partial charges on the C–H group are one third those on the N–H group (the
37 subject of this paper), suggesting that the interaction studied by Brandl et al. is correspondingly weaker. Another survey of note
38 was performed by Weiss et al. in 2010.(Weiss et al., 2001) This complete hydrogen bond analysis of two high resolution protein
39 structures from PDB found 50 C–H π and two (N,O)–H π bonds.

40 In addition to their ubiquity, there is some indication of the importance of these interactions. In a 1993 review, Perutz (Perutz,
41 1993) indicated the potentially wide-ranging importance of these interactions, particularly Armstrong et al.’s demonstration of
42 their role in stabilizing α -helices(Armstrong et al., 1993). There is also evidence that similar interactions play an important role in
43 protein-ligand complexes.(Panigrahi and Desiraju, 2007; Polverini et al., 2008)

44 Following the example of Tüchsen and Woodward (Tüchsen and Woodward, 1987) we seek to use NMR to provide corroborative
45 evidence of aromatic hydrogen bonds. In this paper, we survey the Biological Magnetic Resonance Bank (BMRB) for unusual
46 amide proton chemical shifts and amide-aromatic nuclear Overhauser effects.

47
48 Theoretical models for the geometrical dependence of the ring current shift include parameterization of quantum-mechanical(Haigh
49 and Mallion, 1979; Memory, 1963) calculations, semi-classical approximation using the Biot-Savart Law(Jackson, 1999) for the
50 field arising from current loops (Waugh and Fessenden, 1957; Jr. and Bovey, 1958), and a dipole approximation. For distances
51 from the ring center that are greater than 3 Å above the plane of the ring, and 5 Å in the plane of the ring, the theories all agree
52 well with a dipole approximation.(Hoch, 1983) The $(1-3\cos^2(\theta))/r^3$ geometrical dependence of the field arising from a magnetic
53 dipole (where θ is the angle between the vector from a proton to the aromatic ring center and the vector normal to the plane of the
54 ring) provides vivid explanation for cone separating upfield-shifted from down-field-shifted regions defined by $\theta=54.7^\circ$ (Figure
55 1).



56

57 **Figure 1.** Definition of the azimuthal angle (θ) and demarcation of regions of upfield and downfield ring current shifts.

58 For protons above the plane of a Tyr or Phe ring the upfield shift can reach 1.5 ppm for distances from the ring center around 3

59 Å; for protons in the plane of the ring the downfield shift approaches 2 ppm at 3 Å. For Trp the effects can be significantly larger.

60

61

63 2 Approach

64 To investigate the connection between amide proton chemical shifts and the potential for hydrogen bonding to an aromatic ring,

65 we searched BMRB for assigned amide protons in proteins corresponding to structures deposited in the PDB. BMRB provides the

66 list of BMRB and PDB entry id pairs via BMRB API (http://api.bmrbl.io/v2/mappings/bmrbl/pdb?match_type=exact). As of Jan

67 2021 we found 7750 BMRB/PDB paired entries and retrieved the BMRB entries (in NMR-STAR format (Ulrich et al., 2019)) and

68 PDB entries (in mmCIF format (Bourne et al., 1997)) from their respective databases. We filtered out DNA/RNA entries, entries

69 with legends, oligomers and protein complexes. At the end we prepared a dataset consists of 363686 amide protons from 4670

70 entries. We combined the chemical shift information from BMRB and the geometric information form PDB for each amide proton

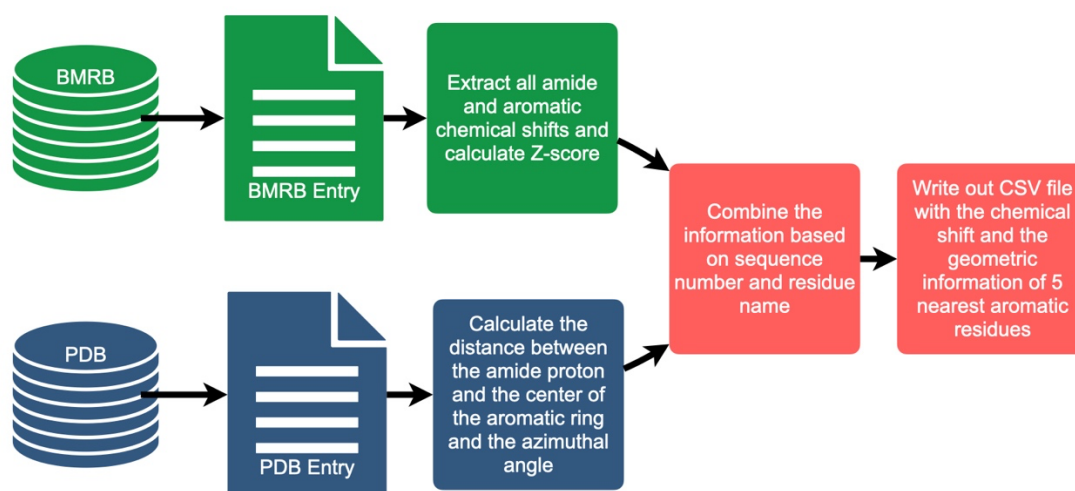
71 and its nearest aromatic ring using sequence number and residue name. For each assigned amide chemical shift, Z-score was

72 computed characterizing the deviation of the shift from its mean value from the BMRB database

$$Z = \frac{\delta_{res} - \bar{\delta}_{res}}{\sigma_{res}} \quad (1)$$

74

75 where δ_{res} is the amide chemical shift of a given residue in ppm, $\bar{\delta}_{res}$ and σ_{res} are the mean and the standard deviation of the amide
76 proton of a given residue type, based on statistics maintained by BMRB (https://bmrbl.io/ref_info/stats.php?restype=aa&set=filt).
77 For each assigned amide, the distance from the amide position to the centre of the nearest aromatic ring is computed from the
78 coordinates in the PDB mmCIF file. The distance is defined as the average of the distance from the amide proton to the centre of
79 the aromatic ring, averaged over the members of the structural ensemble present in the PDB entry. For the nearest aromatic ring,
80 we calculated an azimuth angle (Figure 1), defined as the angle between a vector normal to the aromatic ring plane and the vector
81 between the amide proton and the centre of the ring. The ring normal vector is computed by calculating the cross product of two
82 vectors on the plane of the ring (say the vector from the centre of the ring to CG and CD1). The table of assigned chemical shifts,
83 Z-scores, distances to the nearest aromatic ring and azimuth angles is provided as a comma-separated text file (CSV file) in the
84 supplementary information. The workflow used in the analysis is depicted in Figure 2.



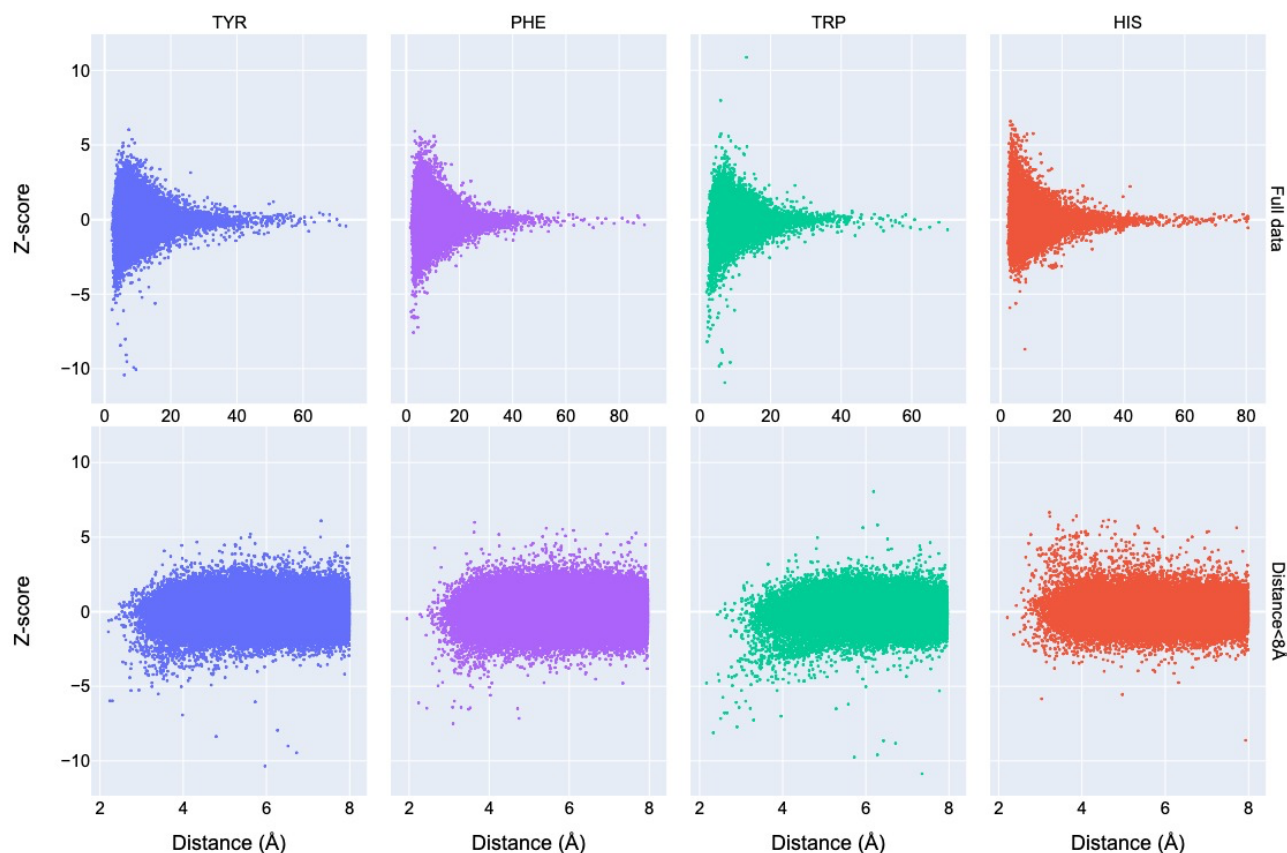
85

86 **Figure 2:** Manual federation of BMRB and PDB via a customized workflow.

87 Corroboration of close proximity between an amide proton and an aromatic ring observed in PDB structures is found in assigned
88 distance restraints based on nuclear Overhauser effects (NOEs) present in the BMRB entries. NMR restraint files from the PDB
89 were parsed using PyNMRSTAR (Smelter et al., 2017) for NOE restraints between amide protons and aromatic ring protons of
90 different residues. Because many files list NOEs under ‘simple’ distance restraints, these were included. Due to inconsistencies
91 prevalent in the restraint data, several criteria were implemented to ensure some conformity in the restraints included in our
92 analysis. This and other reasons for excluding entries from the restraints analysis are described in greater detail in Supplementary
93 Table 1. Also discarded were individual distance restraints which reported only a lower distance bound or an upper distance bound
94 greater than 6Å (as this is inconsistent with the nuclear Overhauser effect) and restraints that were ambiguously between more than
95 two different residues (in order to simplify the analysis). Of the entries that remained, 2573 listed at least one restraint between an
96 amide proton and an aromatic ring proton and 848 did not. For this section of the analysis, the June 2021 ReBoxitory data lake
97 snapshots of BMRB and PDB available on NMRbox (NMRbox.org, /reboxitory/2021/06) were used.

99 3.1 Analysis of Chemical Shift Data

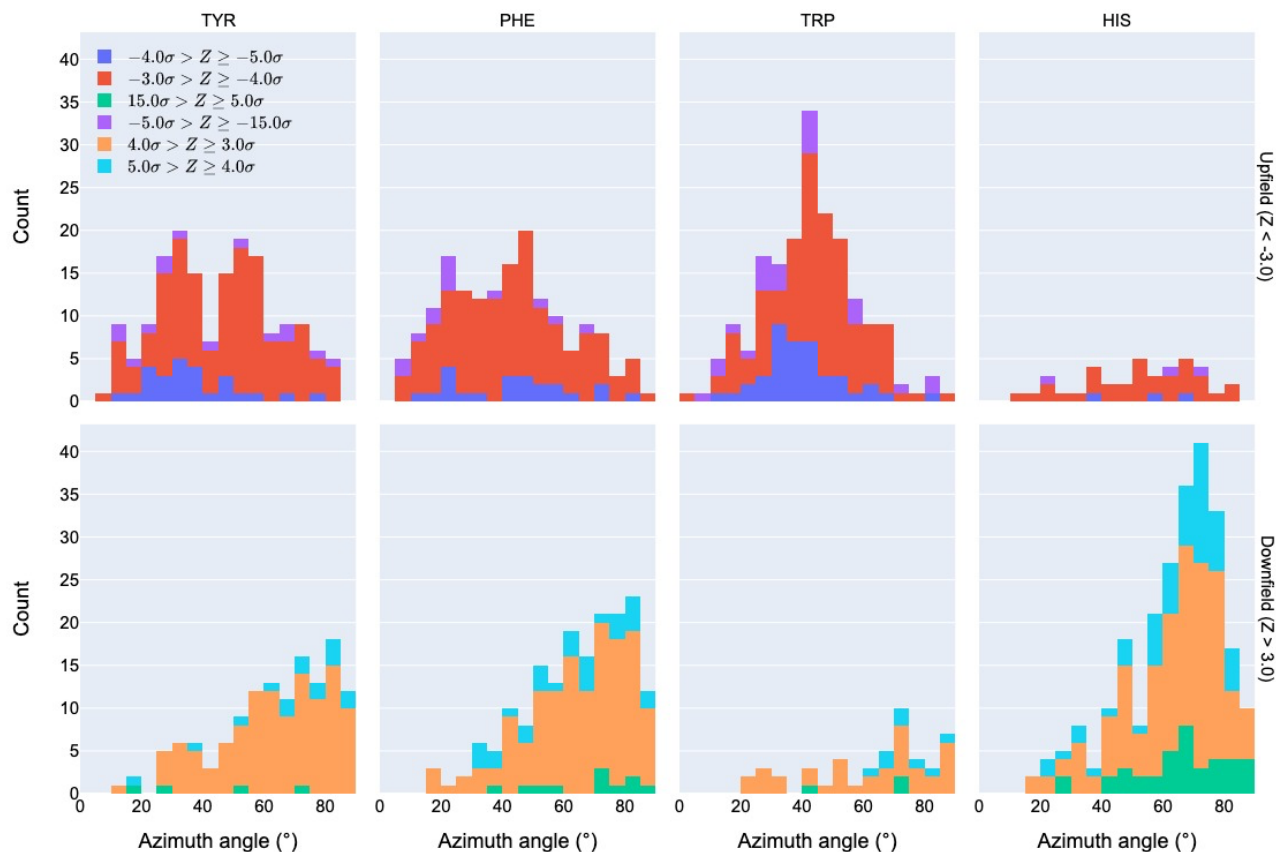
100 Chemical shift Z-scores as a function of distance to the nearest aromatic ring are shown in Figure 3, separated by the type of
 101 aromatic sidechain. For all four aromatic residue types, there is a clear correlation between proximity to the aromatic ring and the
 102 amide chemical shift variance: significant deviations from the mean, corresponding to Z-scores greater than 2, are most likely
 103 when the proton is proximal to an aromatic ring, and the magnitude of the shift deviations are larger for closer proximity. The
 104 bottom row in Figure 3 examines the distribution of amide chemical shifts that are closer than 8 Å in greater detail.



105
 106 **Figure 3:** The distribution of amide chemical shifts as function of the distance of the amide proton from the center of the nearest
 107 aromatic ring.

108
 109 The figure illustrates differences in the pattern of chemical shift deviation for the four different types of aromatic sidechains. For
 110 amide protons proximal to Phe, Tyr, or Trp sidechains, there is a noticeable preponderance of upfield shifts (negative Z-score). In
 111 contrast, His amide protons exhibiting large deviations from the mean tend to be shifted downfield (positive Z-scores). The
 112 difference in behavior of the outliers for the different aromatic residue types suggests the deviations are not simply the result of
 113 residues buried in the protein interior. The upfield-shifted resonances for amides proximal to Phe, Tyr, and Trp are consistent with
 114 hydrogen bonding between the amide and the p - π electrons. The downfield-shifted resonances for amides proximal to His are
 115 consistent with hydrogen bonding to the electronegative nitrogen atoms of the His ring. In-plane downfield ring current shifts are
 116 the same sign as the expected downfield shifts arising from hydrogen bonding, with a predicted amide proton ring current shift of

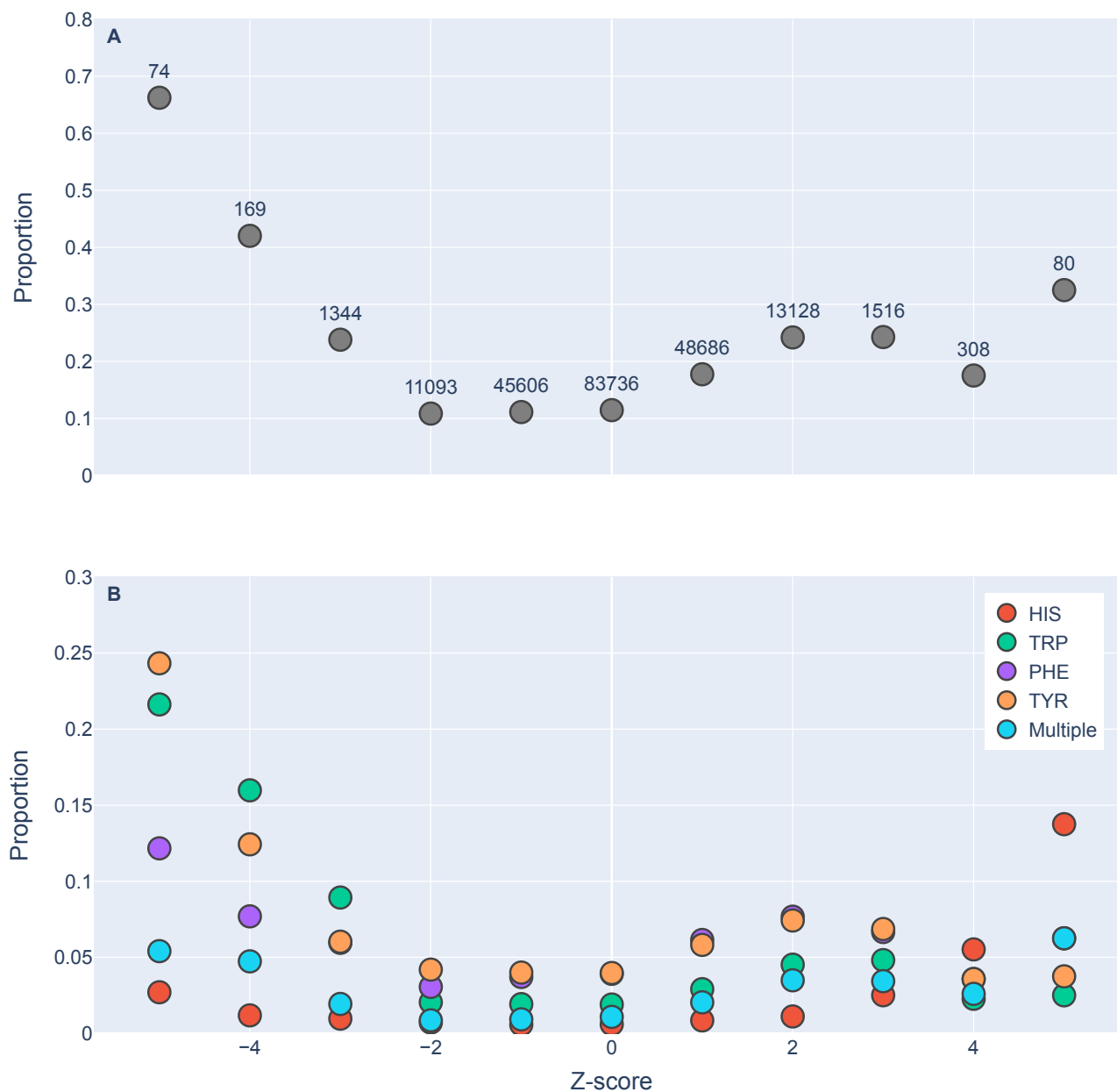
117 0.5 ppm for an amide nitrogen distance of 3.4 Å. This is consistent with the observation of larger magnitude Z scores for downfield-
118 shifted amide protons proximal to His.



119
120 **Figure 4:** Distribution of azimuth angles for outlier ($>3\sigma$) amide proton shifts. Upfield shifts are shown in the top row, downfield
121 shifts in the bottom row.

122
123 Further evidence of the unusual behavior of amide protons with unusual shifts proximal to His and Trp residues is found in their
124 spatial distribution. Figure 4 shows the distribution of azimuth angle for upfield and downfield outliers that are within 8Å of an
125 aromatic ring. (Outliers are defined here as having absolute value of the Z-score greater than 3.) Shift outliers proximal to His tend
126 to reside near the ring plane, whereas shift outliers proximal to Trp tend to reside above the ring plane. Phe and Tyr don't exhibit
127 a pronounced preponderance of outliers above or near the ring plane. Interestingly, none of the maxima in the azimuth angle
128 distributions occur at 0°, expected for an amide proton directly above the ring centroid, nor 90°, expected for an amide proton lying
129 in the ring plane. The peaks near 25° observed for Tyr and Phe are close to the value expected for an amide proton 2.4 Å above
130 the ring plane and directly above one of the ring atoms, rather than above the ring centroid.

131

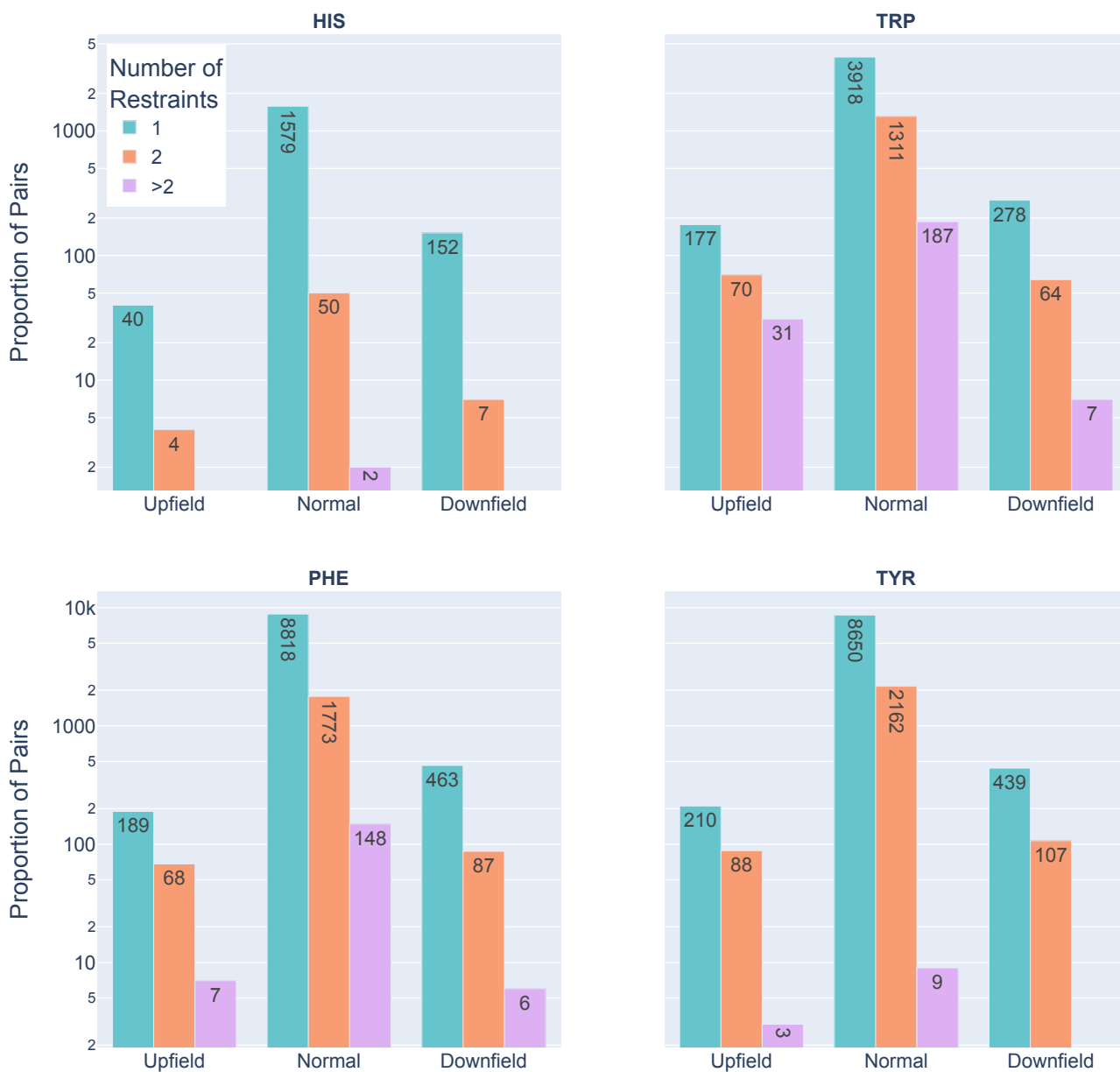


133

134 **Figure 5:** Proportions of amide protons with at least one NOE restraint to an aromatic ring proton (y-axis), as a function of the
 135 Z-score of the amide proton (x-axis). Proportions are calculated with respect to the total number of amide hydrogens with chemical
 136 shifts reported in entries with at least one amide-aromatic restraint. The numbers over each point in panel A are the total number
 137 of such amides (including those lacking any NOE restraints to a nearby aromatic) with that Z-score. In panel B, the restrained
 138 amide protons are further demarcated by the type of aromatic sidechain to which they are restrained.

139

140 We found 31,859 amide protons with at least one NOE restraint to a nearby aromatic ring. Figure 5A shows the proportion of
141 amide protons (from entries with usable restraint data and at least one amide-aromatic restraint) exhibiting these restraints. For
142 both upfield- and downfield-shifted amide protons, the greater the deviation from the mean the greater the likelihood that
143 corresponding NOE restraints are observed. The trend is noticeably more pronounced for the upfield-shifted amide protons, which
144 is consistent with the formation of hydrogen bonds between the amide and the p- π electrons. The downfield-shifted amides exhibit
145 a weaker correlation, which may be indicative of other dominating effects (not necessarily due to nearby aromatic rings). Figure
146 5B further demarcates the data by the type of the nearby aromatic residue. We observe that the preponderance of amide-aromatic
147 restraints in upfield-shifted amide protons for interactions with Trp and Tyr (and to a lesser extent Phe). In contrast, amide protons
148 proximal to His residues predominate strong downfield shifts ($Z \geq 4$). This stands as further evidence for hydrogen bonding from
149 the amide to the p- π electrons in Trp, Tyr, and Phe, and to the nitrogen atoms in the His ring.



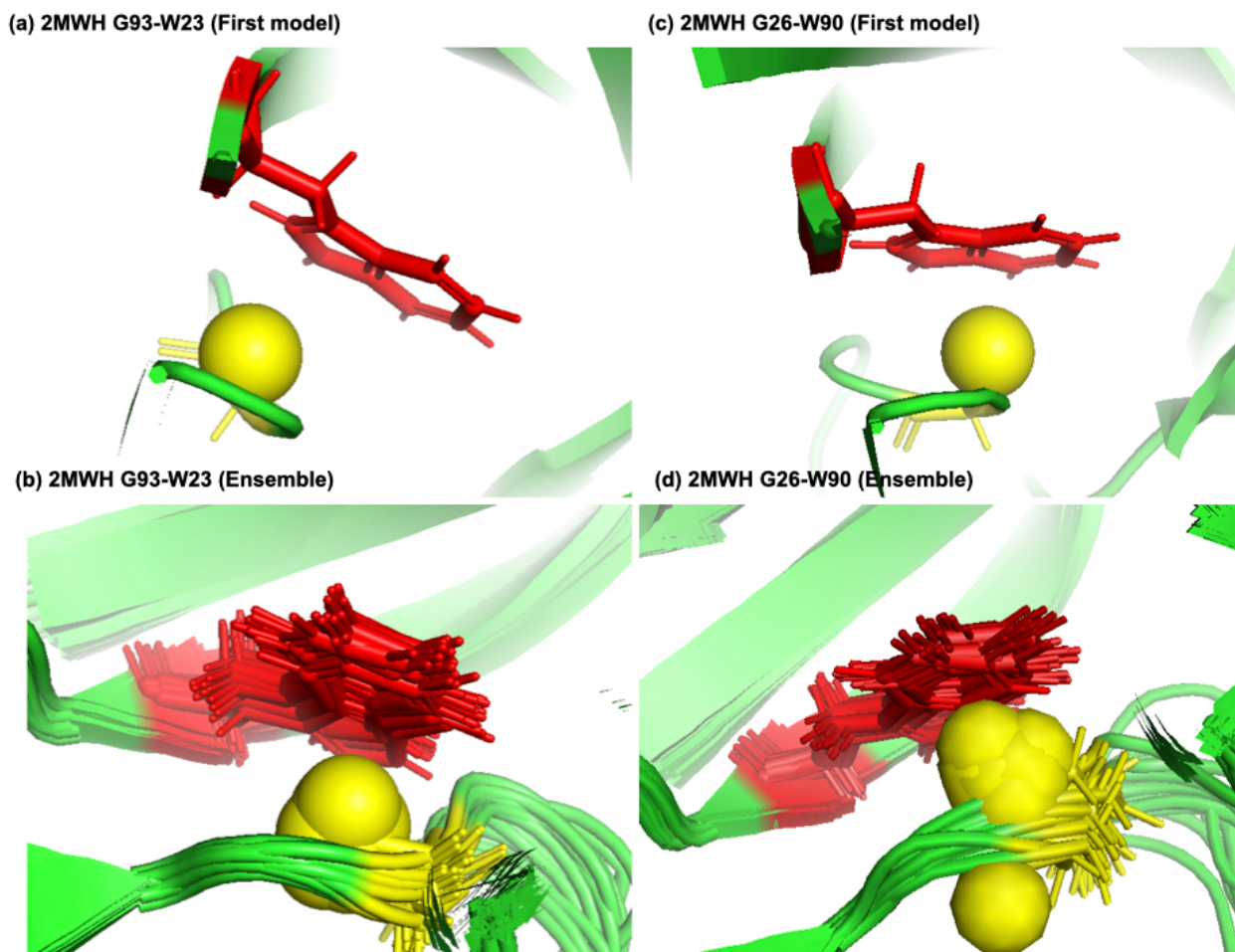
150
 151 **Figure 6:** Shown are the number of restrained amide-aromatic pairs (that is amide protons and aromatic rings with at least one
 152 defined restraint between them) for the four aromatic residue types and three Z-score classifications: upfield ($Z \leq -2$), downfield
 153 ($Z \geq 2$), and normal ($-2 \leq Z \leq 2$). The colors of the bars correspond to the number of restraints between the pairs; bar heights
 154 are plotted using a logarithmic scale.

155
 156 In Figure 6 the restrained amide-aromatic pairs are separated by the type of the aromatic residue and the number of restraints
 157 between the amide proton and the aromatic ring protons. For every aromatic type, a greater proportion of the upfield-shifted pairs
 158 have more than one restraint between them than the downfield-shifted pairs, which may indicate a hydrogen bond from the amide

159 to the p- π electrons. his observation is consistent with the others. Finally, the prevalence of defined restrained pairs with an upfield
160 outlier amide is quite high. From the 2529 entries considered, there were 887 such pairs, more than one in every three entries.

161 3.3 Examples

162

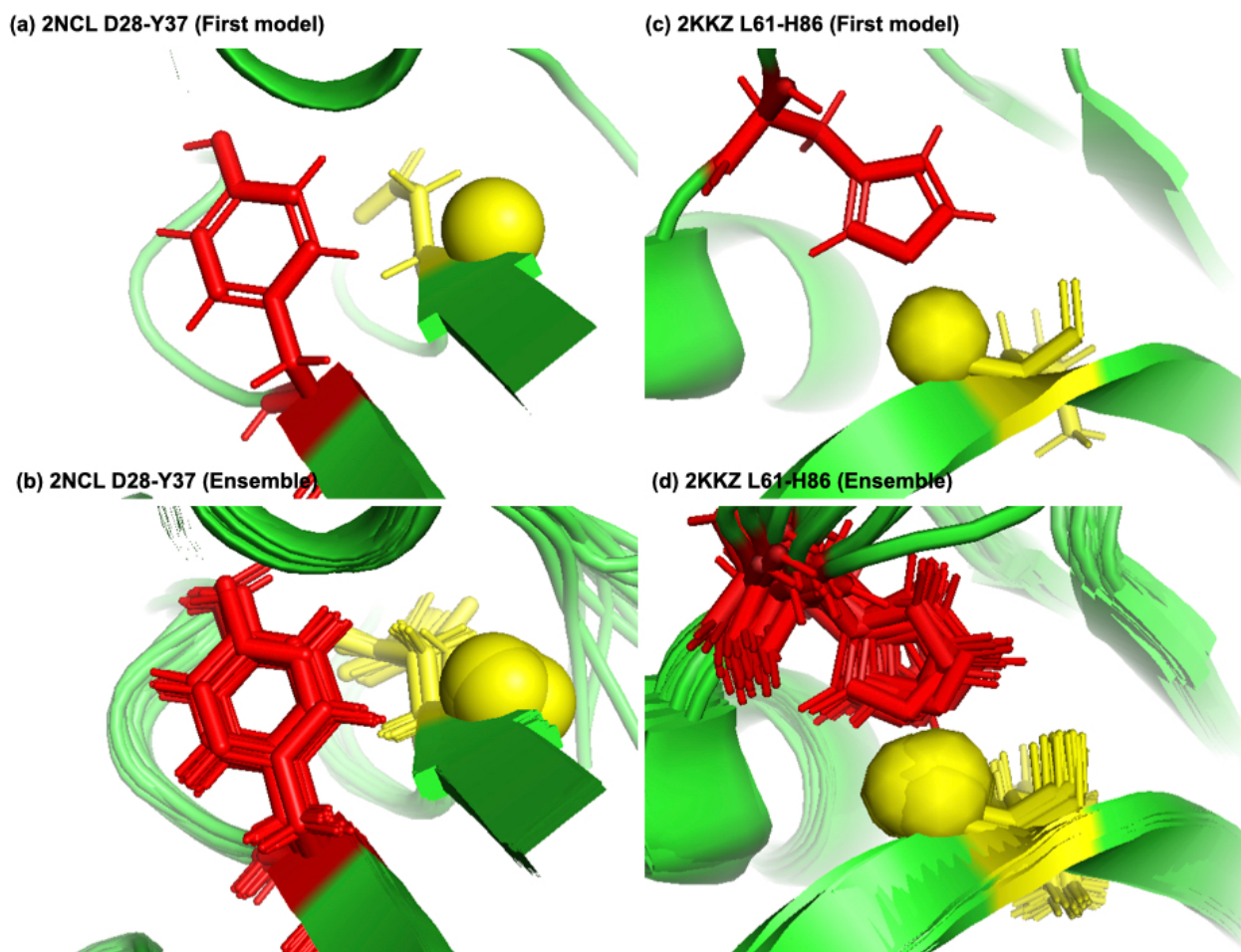


163

164 **Figure 7:** Examples of amide protons with extreme upfield shifts (a,b) PDB:2MWH The G93 amide proton is directly below the
165 W23 aromatic ring ($Z = -7$, $\delta_{GLY} = 2.937$ ppm, $d = 3.99\text{\AA}$, $\theta = 43.9^\circ$, $\bar{\delta}_{GLY} = 8.237$ ppm, $\sigma_{GLY} = 0.770$ ppm), (c,d) PDB:2MWH
166 The G26 amide proton is directly below the W90 aromatic ring ($Z = -6.43$, $\delta_{GLY} = 3.38$ ppm, $d = 2.98\text{\AA}$, $\theta = 25.0^\circ$, $\bar{\delta}_{GLY} =$
167 8.327 ppm, $\sigma_{GLY} = 0.770$ ppm). The amide proton is represented as a yellow sphere and the aromatic side chain is shown in
168 red

169

170 Figure 7a & 7b shows the examples of p- π hydrogen bond in the anti-HIV lectin *Oscillatoria agardhii* agglutinin (PDB ID:2MWH)
171 in which the amide chemical shifts of G93 (z-score = -7, $\delta_H = 2.937$ ppm) and G26 (z-score = -6.43, $\delta_H = 3.38$ ppm) are upfield
172 shifted due to the interaction of W23 and W90 respectively.



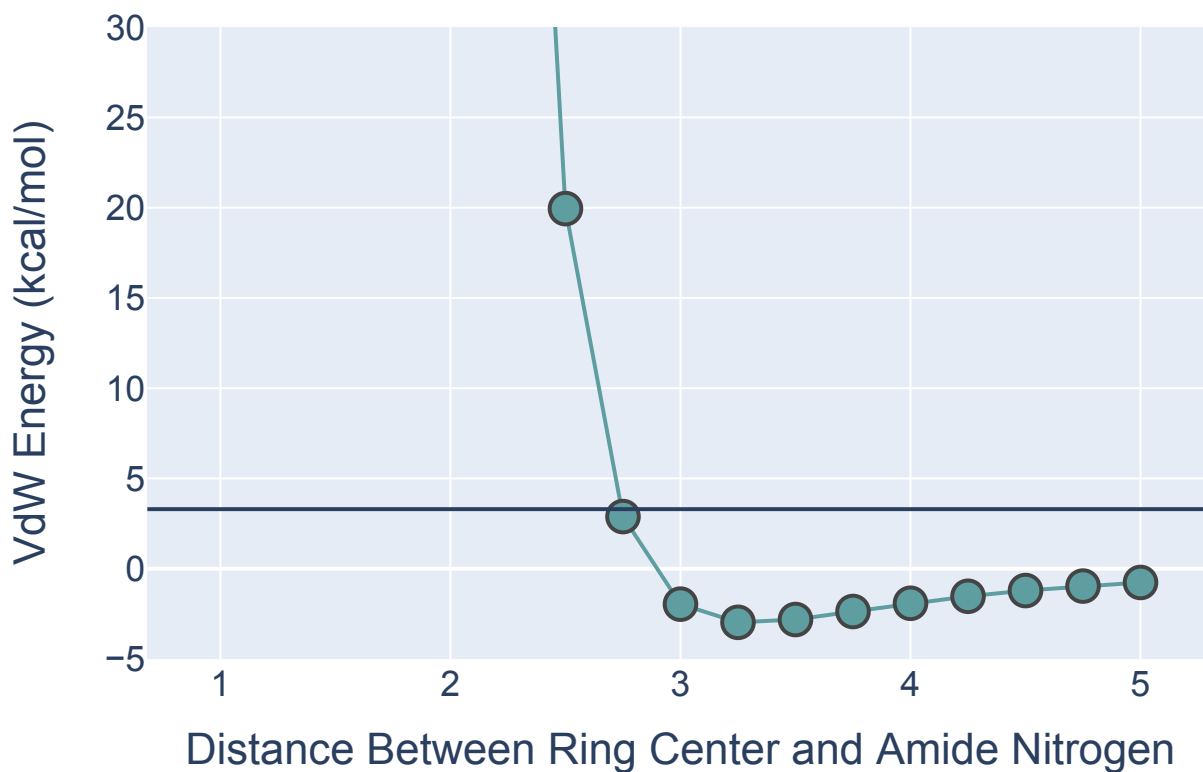
173
 174 **Figure 8:** Examples of amide protons with extreme downfield shifts. (a,b) PDB:2NCL The D28 amide proton is near the plane of
 175 Y37 aromatic ring ($Z=5.21$, $\delta_{ASP} = 11.387$ ppm, $d=5.62\text{\AA}$, $\theta=72.0^\circ$, $\bar{\delta}_{ASP} = 8.299$ ppm, $\sigma_{ASP} = 0.588$ ppm), (c,d) PDB:2KKZ
 176 The L61 amide proton forms a hydrogen bond with the side chain nitrogen of H86 ($Z=6.66$, $\delta_{LEU} = 12.56$ ppm, $d=3.22\text{\AA}$, $\theta=69.7^\circ$
 177 , $\bar{\delta}_{LEU} = 8.217$ ppm, $\sigma_{LEU} = 0.735$ ppm). The amide proton is represented as a yellow sphere and the aromatic side chain is
 178 shown in red.

179
 180
 181 Figure 8a shows the amide proton of D28 is more or less on the plane of the Y37 aromatic ring in BOLA3 protein (PDB ID:2NCL)
 182 resulting in the amide chemical shift of D28 ($z\text{-score}=5.21$, $\delta_H = 11.387$ ppm) to shift downfield. Figure 8b shows an example of
 183 possible hydrogen bond between the NE2 of H86 and the amide proton of L61 in NS1 effector domain (PDB ID:2KKZ). As a
 184 result, L61 ($z\text{-score}=6.66$, $\delta_H = 12.66$ ppm) amide chemical shift is strongly downfield shifted.

185 3.4 Bias, Structure, and Dynamics

186 Potential bias in the BMRB and PDB data likely undercounts the occurrence of aromatic hydrogen bonds. Absent assigned NOEs,
 187 the likelihood that an NMR structure will reflect a hydrogen bond to a π cloud of an aromatic ring is low, because the additive
 188 force fields used to refine most NMR structures, such as X-PLOR/CNS, do not capture the favorable interaction energy. To explore

189 the Van der Waals interactions in an H-bonding geometry, we used MoSART(Hoch and Stern, 2003) to simulate ALA approaching
190 PHE with the amide N-H of the former exactly aligned with the ring normal of the latter. The AMBER99 force field(Wang et al.,
191 2000) was used to compute the energy.



192

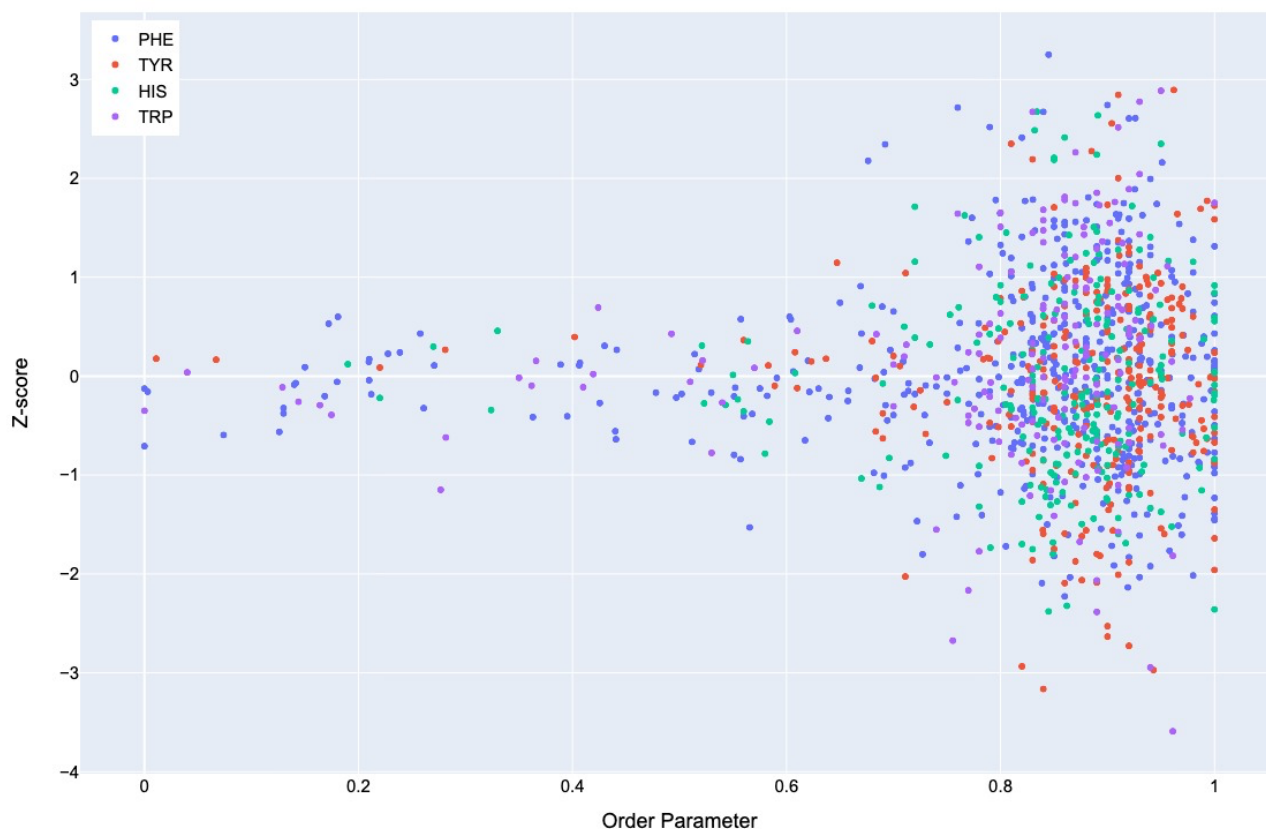
193 **Figure 9:** Van der Waals interaction energies for ALA approaching PHE with its amide N-H aligned with the ring normal. On the
194 x-axis is the distance from the ALA nitrogen to the PHE ring center. VdW interaction energies for each distance were calculated
195 by subtracting the VdW energies of ALA and PHE in isolation from the energies calculated at that distance from one another. All
196 calculations were performed in MoSART using the AMBER99 force field.

197

198 The results, shown in Figure 9, agree with those presented by Levitt and Perutz(Levitt and Perutz, 1988): there is a local minimum
199 in the van der Waals (VdW) energy with the amide nitrogen 3.3 Å from the ring center. The calculations also show that the non-
200 bonded VdW interactions do not preclude adoption of a hydrogen-bonded aromatic ring, however the well depth is so small that
201 the VdW attraction alone is likely insufficient to yield a favorable H-bond geometry without additional restraints.

202 Lack of assignments are not evidence of the absence of an NOE. Missing assignments (for example, 6280 out of 8111 outlying
203 amide proton shifts($|Z|>2$) do not have assigned NOEs to an aromatic ring) also would lead to an undercount. Possible bias in
204 BMRB notwithstanding, such as missing assignments not uniformly distributed, trends in shifts and NOE restraints for different

205 amino acid types that mirror one another provide a form of cross-validation and suggest that the shift outliers are not simply the
206 result of being buried in the protein and thus easier to assign. Bias in PDB NMR structures could reflect current practice in structure
207 refinement, which is dominated by restrained molecular mechanics simulations using empirical force fields augmented with
208 experimental restraint potentials. The forms of these restraint potentials can introduce bias (Hoch and Stern, 2005), and the additive
209 potentials that are used do not explicitly model p- π hydrogen bonds. Absent NOE or ring current restraints, NMR structures are
210 likely to under-represent aromatic hydrogen bonds.



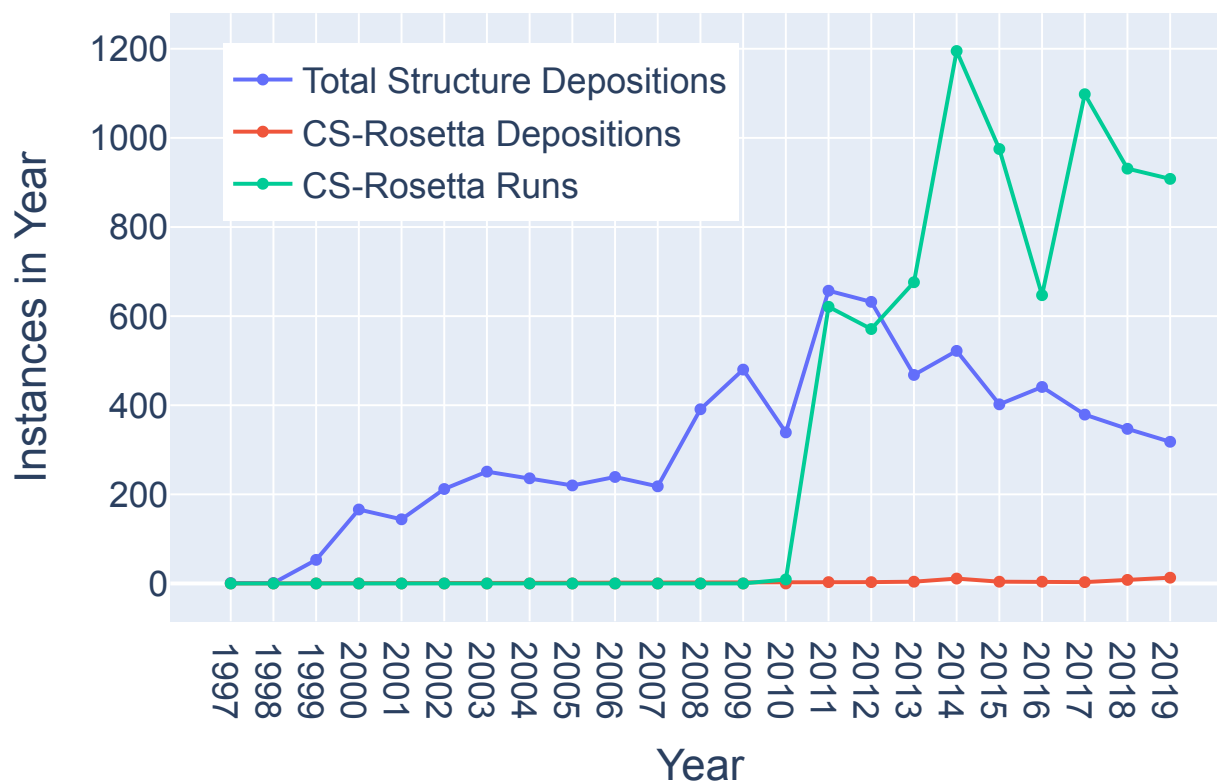
211

212 **Figure 10.** Correlation of Z-scores with order parameters.

213

214 In general, dynamics and disorder render chemical shifts toward their random-coil or median values (Dass et al., 2020; Nielsen
215 and Mulder, 2020). The correlation between secondary shift and order parameters is sufficiently strong that it has been used to
216 predict order parameters from chemical shifts (Figure 10). (Berjanskii and Wishart, 2005) Ring current effects in particular are
217 diminished by fluctuations about the χ_2 torsion angle. (Hoch et al., 1982) Hydrogen bonds involving aromatic rings should diminish
218 these torsional fluctuations and should find correlates in side-chain relaxation properties for aromatic residues. Solution NMR
219 structures in general tend to be more flexible than crystal structures (Fowler et al., 2020), and inclusion of hydrogen bonding
220 interactions between amide groups and aromatic rings could reduce the flexibility and potentially improve the accuracy of NMR
221 structures.

222 Although chemical shifts have been used to refine protein NMR structures (Shen et al., 2009; Berjanskii et al., 2015; Cavalli et al.,
223 2007), for the most part these approaches leverage the influence of backbone torsion angles on chemical shifts, and do not consider
224 the influence of nearby sidechains. Despite evidence that chemical shift refinement software is being used more frequently, the
225 pace of chemical shift-refined structure depositions remains low (Figure 11).

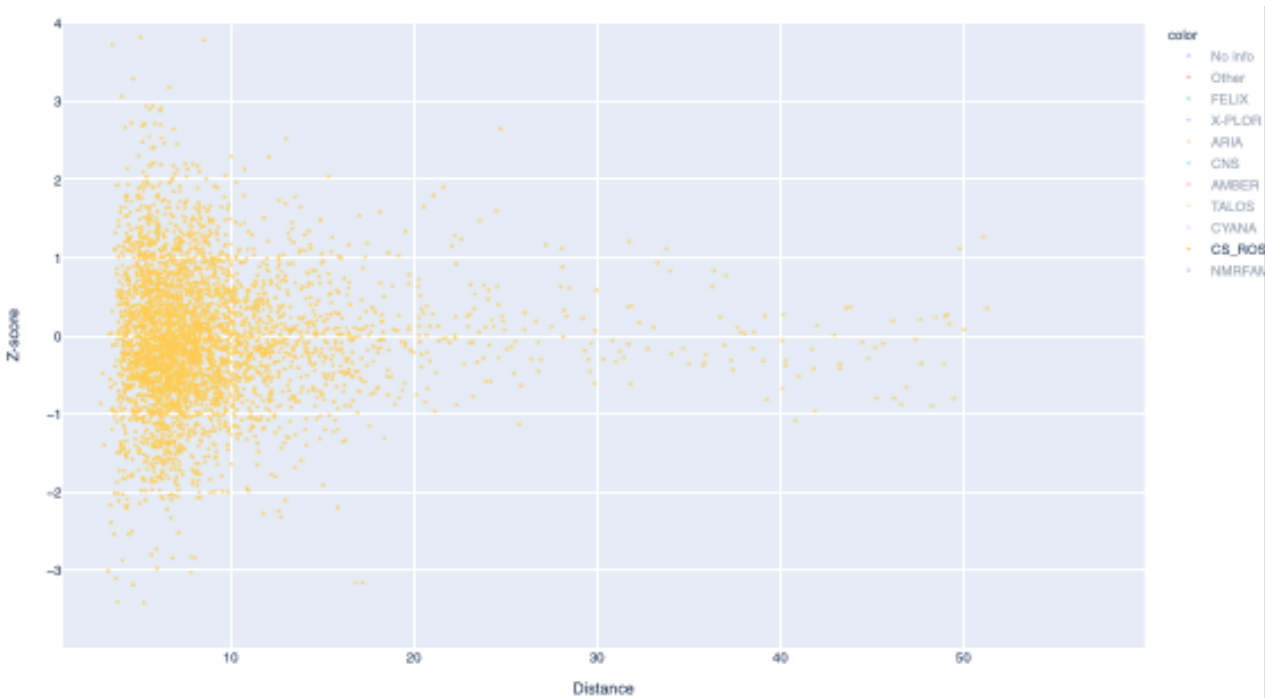


226

227 **Figure 11.** Trends in total BMRB structure depositions (blue), runs executed using the BMRB CS-Rosetta server (green), and
228 depositions citing CS-Rosetta (red).

229

230 Filtering the data plotted in Figure 3 to include only structures that reference CS-Rosetta (Figure 12) does not alter the overall
231 distributions. A challenge confronting a deeper understanding of these effects is that the available metadata in BMRB does not
232 articulate workflows, for example whether CS-Rosetta is used to generate initial trial structures or as a final refinement step), nor
233 does it indicate when ring current shift restraints were utilized.



234

235 **Figure 12.** The distribution of amide chemical shifts for depositions citing C S-Rosetta as function of distance from the center of
 236 the nearest ring (compare Figure 3).

237 4 Concluding Remarks

238 Ring current shifts have a long history of providing structural insights from NMR studies of globular proteins (Perkins and Dwek,
 239 1980), especially for methyl groups, whose secondary shifts tend to be dominated by ring current shifts. Early studies were largely
 240 anecdotal, focusing on individual proteins or small surveys. While relatively dynamic aromatic rings (for example Tyr and Phe
 241 rings that undergo ring flips on the fast exchange time scale) and disorder diminish the influence of ring current effects on secondary
 242 shifts (Hoch et al., 1982), the accumulation of data in BMRB for folded proteins has provided a wealth of amide chemical shifts
 243 exhibiting large secondary chemical shifts. Federation of BMRB chemical shift data with structural data from PDB confirms the
 244 strong correlation between proximity to an aromatic ring and extreme secondary shifts. Markedly different secondary shift trends
 245 for different aromatic residue types suggests promising avenues for improving protein structure determination by NMR. Though
 246 chemical shift refinement has been repeatedly demonstrated (Perilla et al., 2017), it has not yet been widely adopted.

247

248 The extreme outlier amide chemical shifts and corroborating NOE effects examined here provide strong evidence of the widespread
 249 existence of amide-aromatic hydrogen bonds, but they are not fully conclusive. Nonetheless potential for under-representation in
 250 the BMRB data exists because of incomplete assignments. Relaxation studies on ring dynamics, contrasting rings where evidence
 251 suggests the presence of hydrogen bonding with rings lacking such evidence, could provide additional corroboration. Molecular
 252 mechanics simulations and structure refinement using polarizable force fields could reveal additional aromatic hydrogen bonds
 253 and restricted ring dynamics in folded proteins. We have initiated investigations along some of these lines.

254

255 More broadly, this preliminary investigation highlights the potential for unlocking latent knowledge hidden in BMRB, PDB, and
 256 other biological databases. The challenges posed include curation and validation of the data repositories and federation of data

257 between repositories. Robust and efficient solutions to these challenges are needed in order to realize the full promise of emerging
258 methods in Machine Learning. (Hoch, 2019)
259

260 **5 Acknowledgements**

261 This work was supported by a grant from the Miriam and David Donoho Foundation, and by grants from the US National Institutes
262 of Health (R01GM109046; P41GM111135) and from the University of Connecticut Office of the Vice President for Research
263 (CARIC). We thank Milo Westler and Charles Schwieters for helpful discussions. We thank a reviewer for raising the question
264 that led to understanding the significance of the peaks near 25° in the angular distributions.
265

266

267

268

269 **References**

270

- 271 Armstrong, K. M., Fairman, R., and Baldwin, R. L.: The (i, i + 4) Phe-His interaction studied in an alanine-based alpha-
272 helix, *J Mol Biol*, 230, 284-291, 10.1006/jmbi.1993.1142, 1993.
- 273 Berjanskii, M., Arndt, D., Liang, Y., and Wishart, D. S.: A robust algorithm for optimizing protein structures with NMR
274 chemical shifts, *J Biomol NMR*, 63, 255-264, 10.1007/s10858-015-9982-z, 2015.
- 275 Berjanskii, M. V. and Wishart, D. S.: A simple method to predict protein flexibility using secondary chemical shifts, *J*
276 *Am Chem Soc*, 127, 14970-14971, 10.1021/ja054842f, 2005.
- 277 Bourne, P. E., Berman, H. M., McMahon, B., Watenpaugh, K. D., Westbrook, J. D., and Fitzgerald, P. M. D.: The
278 Macromolecular Crystallographic Information File (mmCIF), *Methods in Enzymology*, 277, 571-590, 1997.
- 279 Brandl, M., Weiss, M. S., Jabs, A., Sühnel, J., and Hilgenfeld, R.: C-H...pi-interactions in proteins, *J Mol Biol*, 307, 357-
280 377, 10.1006/jmbi.2000.4473, 2001.
- 281 Brinkley, R. L. and B., G. R.: Hydrogen bonding with aromatic rings., *AIChE Journal*, 47, 948-953, 2001.
- 282 Burley, S. K. and Petsko, G. A.: Amino-aromatic interactions in proteins, *FEBS Lett*, 203, 139-143, 10.1016/0014-
283 5793(86)80730-x, 1986.
- 284 Cavalli, A., Salvatella, X., Dobson, C. M., and Vendruscolo, M.: Protein structure determination from NMR chemical
285 shifts, *Proceedings of the National Academy of Sciences of the United States of America*, 104, 9615-9620,
286 10.1073/pnas.0610313104, 2007.
- 287 consortium, w.: Protein Data Bank: the single global archive for 3D macromolecular structure data, *Nucleic Acids*
288 *Res*, 47, D520-D528, 10.1093/nar/gky949, 2019.
- 289 Dass, R., Mulder, F. A. A., and Nielsen, J. T.: ODINPred: comprehensive prediction of protein order and disorder, *Sci*
290 *Rep*, 10, 14780, 10.1038/s41598-020-71716-1, 2020.
- 291 Fowler, N. J., Sljoka, A., and Williamson, M. P.: A method for validating the accuracy of NMR protein structures, *Nat*
292 *Commun*, 11, 6321, 10.1038/s41467-020-20177-1, 2020.
- 293 Haigh, C. W. and Mallion, R. B.: Ring current theories in nuclear magnetic resonance, *Progress in Nuclear Magnetic*
294 *Resonance Spectroscopy*, 13, 303-344, [https://doi.org/10.1016/0079-6565\(79\)80010-2](https://doi.org/10.1016/0079-6565(79)80010-2), 1979.
- 295 Hoch, J. C.: The Influence of Protein Structure and Dynamics on NMR Parameters, *Chemistry*, Harvard University,
296 1983.
- 297 Hoch, J. C.: If machines can learn, who needs scientists?, *J Magn Reson*, 306, 162-166, 10.1016/j.jmr.2019.07.044,
298 2019.
- 299 Hoch, J. C. and Stern, A. S.: MoSART [code], 2003.
- 300 Hoch, J. C. and Stern, A. S.: Bayesian Restraint Potentials for Consistent Inference of Biomolecular Structure from
301 NMR Data, 2005.
- 302 Hoch, J. C., Dobson, C. M., and Karplus, M.: Fluctuations and averaging of proton chemical shifts in the bovine
303 pancreatic trypsin inhibitor, *Biochemistry*, 21, 1118-1125, 1982.
- 304 Jackson, J. D.: *Classical Electrodynamics*, 3rd, Wiley1999.
- 305 Jr., C. E. J. and Bovey, F. A.: Calculation of Nuclear Magnetic Resonance Spectra of Aromatic Hydrocarbons, *The*
306 *Journal of Chemical Physics*, 29, 1012-1014, 10.1063/1.1744645, 1958.
- 307 Klemperer, W., Cronyn, M. W., Maki, A. H., and Pimentel, G. C.: Infrared studies of the association of secondary
308 amides in various solvents., *J. Amer. Chem. Soc.*, 76, 5846-5848, 1954.
- 309 Knee, J. L., Khundkar, R. L., and Zewail, A. H.: Picosecond photofragment spectroscopy. iii. vibrational
310 predissociation of van der waals' clusters., *J. Chem. Phys.*, 87, 115-127, 1987.
- 311 Levitt, M. and Perutz, M. F.: Aromatic rings act as hydrogen bond acceptors, *J Mol Biol*, 201, 751-754, 1988.

312 McPhail, A. T. and Sim, G. A.: Hydroxyl–benzene hydrogen bonding: an x-ray study., *Chem. Comm.*, 7, 124-126,
313 1965.

314 Memory, J. D.: Ring Currents in Pentacyclic Hydrocarbons, *The Journal of Chemical Physics*, 38, 1341-1343,
315 10.1063/1.1733855, 1963.

316 Nielsen, J. T. and Mulder, F. A. A.: Quantitative Protein Disorder Assessment Using NMR Chemical Shifts, *Methods*
317 *Mol Biol*, 2141, 303-317, 10.1007/978-1-0716-0524-0_15, 2020.

318 Panigrahi, S. K. and Desiraju, G. R.: Strong and weak hydrogen bonds in the protein-ligand interface, *Proteins*, 67,
319 128-141, 10.1002/prot.21253, 2007.

320 Perilla, J. R., Zhao, G., Lu, M., Ning, J., Hou, G., Byeon, I. L., Gronenborn, A. M., Polenova, T., and Zhang, P.: CryoEM
321 Structure Refinement by Integrating NMR Chemical Shifts with Molecular Dynamics Simulations, *J Phys Chem B*,
322 121, 3853-3863, 10.1021/acs.jpcc.6b13105, 2017.

323 Perkins, S. J. and Dwek, R. A.: Comparisons of ring-current shifts calculated from the crystal structure of egg white
324 lysozyme of hen with the proton nuclear magnetic resonance spectrum of lysozyme in solution, *Biochemistry*, 19,
325 245-258, 1980.

326 Perutz, M. F.: The role of aromatic rings as hydrogen-bond acceptors in molecular recognition., *Phil. Trans. Royal*
327 *Soc., Series A: Phys. and Eng. Sci.*, 345, 105-112, 1993.

328 Plevin, M. J., Bryce, D. L., and Boisbouvier, J.: Direct detection of CH/pi interactions in proteins, *Nat Chem*, 2, 466-
329 471, 10.1038/nchem.650, 2010.

330 Polverini, E., Rangaraj, G., Libich, D. S., Boggs, J. M., and Harauz, G.: Binding of the proline-rich segment of myelin
331 basic protein to SH3 domains: spectroscopic, microarray, and modeling studies of ligand conformation and effects
332 of posttranslational modifications, *Biochemistry*, 47, 267-282, 10.1021/bi701336n, 2008.

333 Shen, Y., Vernon, R., Baker, D., and Bax, A.: De novo protein structure generation from incomplete chemical shift
334 assignments, *J Biomol NMR*, 43, 63-78, 10.1007/s10858-008-9288-5, 2009.

335 Smelter, A., Astra, M., and Moseley, H. N.: A fast and efficient python library for interfacing with the Biological
336 Magnetic Resonance Data Bank, *BMC Bioinformatics*, 18, 175, 10.1186/s12859-017-1580-5, 2017.

337 Tüchsen, E. and Woodward, C.: Assignment of asparagine-44 side-chain primary amide 1H NMR resonances and the
338 peptide amide N1H resonance of glycine-37 in basic pancreatic trypsin inhibitor, *Biochemistry*, 26, 1918-1925,
339 10.1021/bi00381a020, 1987.

340 Ulrich, E. L., Baskaran, K., Dashti, H., Ioannidis, Y. E., Livny, M., Romero, P. R., Maziuk, D., Wedell, J. R., Yao, H.,
341 Eghbalnia, H. R., Hoch, J. C., and Markley, J. L.: NMR-STAR: comprehensive ontology for representing, archiving and
342 exchanging data from nuclear magnetic resonance spectroscopic experiments, *J Biomol NMR*, 73, 5-9,
343 10.1007/s10858-018-0220-3, 2019.

344 Wang, Junmei, Ciepla, Piotr, Kollman, and A., P.: How well does a restrained electrostatic potential (RESP) model
345 perform in calculating conformational energies of organic and biological molecules?, *J. Comp. Chem.*, 21, 1049-
346 1074, 2000.

347 Waugh, J. S. and Fessenden, R. W.: Nuclear Resonance Spectra of Hydrocarbons: The Free Electron Model, *Journal*
348 *of the American Chemical Society*, 79, 846-849, 10.1021/ja01561a017, 1957.

349 Weiss, M. S., Brandl, M., Sühnel, J., Pal, D., and Hilgenfeld, R.: More hydrogen bonds for the (structural) biologist,
350 *Trends Biochem Sci*, 26, 521-523, 10.1016/s0968-0004(01)01935-1, 2001.

351